ANALYSIS OF THE EGNOS IONOSPHERIC MODEL AND ITS IMPACT ON THE INTEGRITY LEVEL IN THE CENTRAL EASTERN EUROPE REGION

B. Lupsic [1], B. Takács [1]

[1] Department of Geodesy and Surveying, Faculty of Civil Engineering, Budapest University of Technology and Economics, Hungary - (lupsic.balazs, takacs.bence)@epito.bme.hu

Commission IV, WG IV/4

KEYWORDS: GNSS, EGNOS, CODE, Ionosphere, Model Comparison, Integrity, Protection Level

ABSTRACT

The demand for Global Navigation Satellite System in safety-related applications has rapidly increased in the last few years. The foreseeable release of self-driving cars is already showing the importance of the integrity concept of satellite-based navigations. Correction services as EGNOS can actively improve the integrity assurance build up. The paper aims the examination of the EGNOS ionospheric model concerning integrity. The focus is on the Eastern European area are close to the east edge of the EGNOS coverage area. We processed the available EGNOS data from 2018 and compared the performance of the ionospheric correction with a profoundly credible model. The paper presents the basic statistical properties of the comparison focusing on deviances, which could lead to navigation integrity. The article has an additional focus on how the quality of the EGNOS ionosphere model can influence the Protection Level in the eastern region. Satellites with low elevation angle may be out of the EGNOS coverage area, and the absence of these transmitters can negatively affect the Protection Level. The paper shows the quality and quantity of the above mentioned negative impact with the help of real life and simulated data.

1. INTRODUCTION

For the past two decades, there has been an accelerated rise in the use of GNSS technologies. GNSS applications have attracted interest from the aviation field in the ‘90s. With the advent of smartphones, the GNSS navigation became part of our daily lives. We are at the edge of Industry 4.0 and self-driving cars, which may give another considerable push to the GNSS related researches and developments. The market allows numerous navigation solution which varies in cost, size, endurance, accuracy, and reliability. Many affordable receivers could handle multi-frequencies and multi-constellation however, a significant share of GNSS equipment still process on single frequencies.

One of the major error factors of a single frequency receiver is the ionospheric delay, which is proportional to the total electron content (TEC) along the path from the satellite to a receiver. For example, 1 TECU will introduce a pseudorange delay of 0.163 meters and 0.267 meters in L1 and L2 frequencies, respectively. The elimination or correction of the ionospheric signal delay is a necessary measure to reach submeter accuracies in GNSS based navigation systems. The focus of the current paper is on the EGNOS (European Geostationary Navigation Overlay Service) ionospheric model. EGNOS is the regional satellite-based augmentation system (SBAS) of Europe that is used to improve the performance of global navigation satellite systems (GNSSs), such as GPS and Galileo. It has been deployed to provide safety of life navigation services to aviation, maritime and land-based users over most of Europe.

The Safety of Life (SoL) service of EGNOS is compliant with the aviation requirements for Approaches with Vertical Guidance (APV-I) and Category I precision approaches, as defined by ICAO in Annex 10 [7] [14]. At the edge of the coverage area, the integrity performance of EGNOS was examined by many papers [6] [9] [10]. A comparative study could highlight the ionospheric effect on integrity [8] [13]. In addition to the ionospheric delay, other systematic errors have a significant impact on the integrity level, like the tropospheric delay. [19].

The EGNOS's model could be compared to a more reliable post processed model, namely to the Global Ionosphere Maps produced by CODE (Center for Orbit Determination in Europe) Analysis Center operated by AIUB (Astronomical Institute University of Bern). One of the main guesswork is that the CODE model could be handled as a reference ionospheric model which would account for the real unbiased ionospheric delay.

2. IONOSPHERIC MODELS

The ionospheric effect plays a significant impact on the accuracy of the single frequency receivers. The position bias caused by the uncompensated delay ranges from meter level to several ten meters in extreme conditions. During the design of the GPS constellation the constructors were aware of the role of the ionosphere as an error source, and to mitigate this effect, the Klobuchar model had become a fundamental part of the GPS [4]. A great advantage of the model is the six broadcasted parameters are sufficient to align the Klobuchar model globally and the processing load of applying the model is low compared to other models like the Galileo equivalent, the NeQuick. On the other hand, using the Klobuchar model can only compensate for approximately 50% - 60% of the ionospheric delay.

The growing number of ionosphere related researches have made a public interest to create a general exchange format for ionospheric measurements. Following the footstep of the Receiver Independent Exchange (RINEX) format, the Ionosphere Map Exchange (IONEX) format had been defined as a standard format for information about the vertical total electron content (VTEC) at specified grid points. One of the most prominent sources of VTEC information is the International GNSS Service (IGS) [3] [12]. The IONEX format makes it easy to compare different vertical total electron content (VTEC) maps to each other.

The ionospheric pierce point (IPP) between the receiver's location and the observed satellite could be calculated based on a single layer model where it is assumed that the TEC is concentrated within an infinitely thin layer at a given height. The VTEC value of the IPP could be determined by an ionospheric model. The elevation of the line of sight (LOS) vector determine the obliquity factor, and this factor transforms the VTEC value to slant total electron content (STEC), which is directly proportional to the ionospheric delay on the GNSS signal.

2.1 CODE model

Besides the EGNOS ionospheric model, the Center for Orbit Determination Europe (CODE) model becomes the focus of our interests [2] [15]. Global ionosphere maps (GIM) are generated daily basis at CODE using data from about 200 GNSS sites of the IGS and other institutions. The vertical total electron content is modeled in a solar-geomagnetic reference frame using a spherical harmonics expansion up to degree and order 15. Piece-wise linear functions are used for representation in the time domain. The time spacing of their vertices is 1 hour, conforming to the epochs of the VTEC maps [2]. The paper presents the results acquired from analyzing the 2018 year data from the AIUB server. The timely and spatially collected and processed root mean square (RMS) data can be found in Table 1. In the 'Global' row, we did not restrict the grid points; however, the European region was defined by longitude -60º – 60º and latitude 10º – 90º.

	Mean	Std	Min	Max	Median
Global	1.4	0.5	0.3	4.7	1.3
Europe	0.7	0.2	0.3	1.4	0.7

Table 1. Statistics of CODE model RMS values in 2018. Values are expressed in TECU.

The averaged RMS in the European region is about half of the already low global RMS driven by the increased density of stations involved in processing (Table 1).

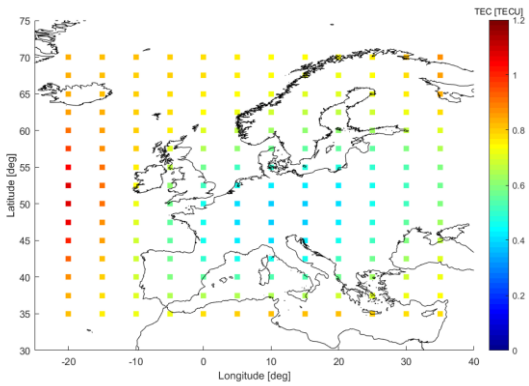

Figure 1. CODE model's annual average RMS values in 2018.

The RMS of the CODE model is between 0.4 – 0.6 TECU in the continental region. The precision of the grid points slightly increases near the map's border (Figure 1).

2.2 EGNOS ionospheric model

The European SBAS system, the EGNOS provides open access corrections in L-band. EGNOS broadcasts Ionospheric Delay Corrections (GIVD) for a set of predefined points defined on a grid 350km above the WGS-84 ellipsoid Earth approximation (IGPs), and their accuracy (σ^2_{GIVE}) in terms of GIVEI (GIVE Indicators) for the IGPs. The broadcasted ionospheric data cyclically refreshed, typically in 1–2 minutes.

The GIVEI values go from 1 to 13 can be converted to variances. The GIVEI value 14 corresponds to the do-not-use message. The applications of the received data are described by the following formulas [5].

$$\sigma^2_{i,UIRE} = F^2_{PP}\sigma^2_{i,UIVE} \quad (1)$$

$$\sigma^2_{i,UIVE} = \sum_{n=1}^{4} W_n(x_{PP}, y_{PP})\,\sigma^2_{n,ionogrid} \quad (2)$$

$$\sigma^2_{n,ionogrid} = \sigma^2_{GIVE} + \varepsilon^2_{iono} \quad (3)$$

where F_{PP} is the obliquity factor (transforms vertical delay to slant), W_n is the weighting function, $\sigma^2_{n,ionogrid}$ is the grid ionospheric vertical error bound with degradation over time, x_{PP}, y_{PP} are the coordinates of interpolation grid points, σ^2_{GIVE} is the grid ionospheric vertical error bound, $\varepsilon^2_{\mathrm{iono}}$ is the degradation of ionospheric correction information.

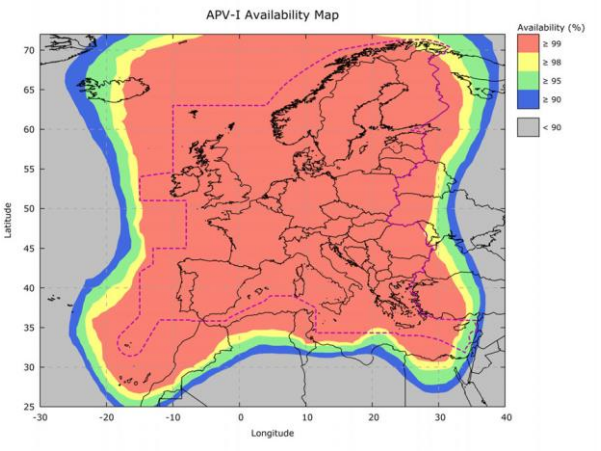

Figure 2. EGNOS availability map [1]

To provide ionospheric correction to the coverage area (Figure 2), the broadcasted VTEC map shall be extended because at low elevation angles the difference between the ionospheric pierce points (IPP), and the location of a user could be as high as 15º–20º.

Total electron Content may vary between 0 and 30 TECU in Europe (Figure 3) while the RMS values in the grid points usually are 4-5 TECU. However, the GIVEI value could correspond to 84 TECU as well (Figure 4).

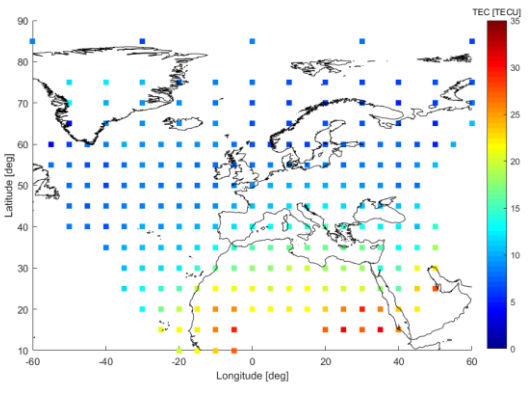

Figure 3. EGNOS TEC map at 13:45 20/08/18

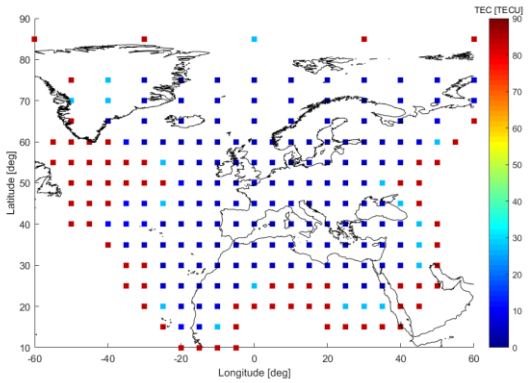

Figure 4. EGNOS RMS map at 13:45 20/08/18.

The RMS map shows how the precision of the model rapidly decreases near the edge (Figure 3 and Figure 4).

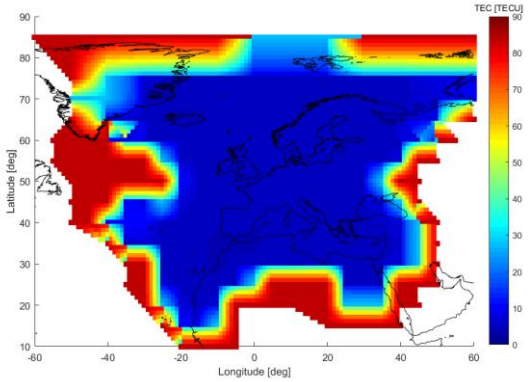

Figure 5. Interpolated EGNOS RMS map at 13:45 20/08/18

As it was examined in the CODE model, the authors collected the 2018 year EMS. Global Integrated Navigation Algorithm (GINA) software was created to process the EMS files and perform statistical analysis (Table 2) [18]. GINA is an open source software and heavily relies on the GPSTK library [17].

Mean	Std	Min	Max	Median
5.0	3.5	3.9	84.2	4.5

Table 2. Statistics of EGNOS model RMS values in 2018. Values are in TECU.

The average of the RMS at the grid points is between 4-5 TECU (Figure 6). The standard deviation of the CODE model is less an order of magnitude than the EGNOSS ionospheric model in the inner territory of the coverage area.

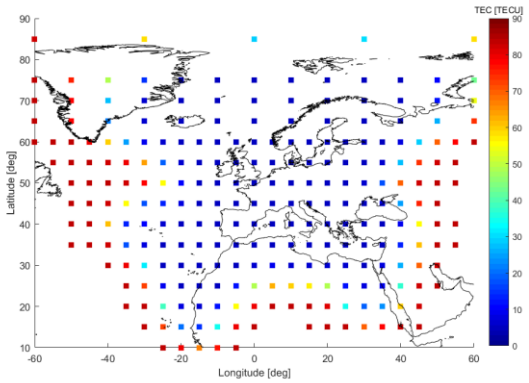

Figure 6. EGNOS model's annual average RMS values

Based on the comparative analysis of the yearly averaged RMS data, the CODE model has been verified as a valid reference model for the target region Europe.
[12].

3. MAXIMUM LIKELIHOOD FOR COMPARISON

The previous section had shown that the CODE model could be used as a reference for the VTEC map comparison. This assumption is supported by the fact that the variance of the CODE yields a tenth of the EGNOS ionospheric model. In the current section, this assumption is neglected for the moment and the question is, how the similarity of the two models could be measured. The authors submit a maximum likelihood-based method to measure the grid wise similarity of two VTEC maps.

Assuming two independent unbiased measurements with corresponding standard deviations finding the best estimation of the real value could be found with Bayesian inference. Without loss of generality, the probability density functions (PDF) of the measurements are Gaussian (Figure 7).

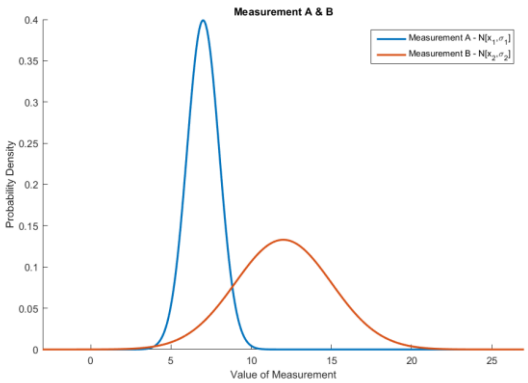

Figure 7. To illustrate the mathematical aspect of the problem. Let assume two independent measurements with a known probability distribution to observe the same value. What is the likeliness that both measures are unbiased?

The prior belief that μ is the real value. Measurement A and B observe this μ value with their corresponding σ_1 and σ_2 standard deviations. The measurement A observes a x_1 value and the measurement B observes a x_2 value. What is the likelihood that both measurements would get the values mentioned above if the observed state value is μ. With notations, this looks the following:

$$P((A{:}\,x_1, B{:}\,x_2)|R{:}\,\mu) = ? \tag{4}$$

The expression can be split using the fact that both A and B measurements are independent of each other.

$$P\big((A{:}\,x_1, B{:}\,x_2)\big|R{:}\,\mu\big) = P(A{:}\,x_1|R{:}\,\mu)P(B{:}\,x_2|R{:}\,\mu) \tag{5}$$

The R shall be chosen to maximize the conditional distribution. To estimate the R-value, one could use the maximum likelihood method in the general case; however, with Gaussian assumption, a weighted least square or Kalman filter could easily estimate the R-value. In the case of Gaussia, the μ would be,

$$\mu = \frac{x_2{\sigma_1}^2 + x_1{\sigma_2}^2}{{\sigma_1}^2 + {\sigma_2}^2} \tag{6}$$

If the μ is known with maximum likelihood, the conditional probability is calculable.

$$MLH := P(A: x_1|R: \mu)P(B: x_2|R: \mu) = N[\mu, \sigma_1]|_{x_1} N[\mu, \sigma_2]|_{x_2} \quad (7)$$

The normalization factor would be the following:

$$NF := P(A: \mu|R: \mu)P(B: \mu|R: \mu) = N[\mu, \sigma_1]|_{\mu} N[\mu, \sigma_2]|_{\mu} \quad (8)$$

After normalization on could get the following:

$$MLH_{Norm} := \frac{MLH}{NF} = \frac{N[\mu, \sigma_1]|_{x_1} N[\mu, \sigma_2]|_{x_2}}{N[\mu, \sigma_1]|_{\mu} N[\mu, \sigma_2]|_{\mu}} \quad (9)$$

This MLH_{Norm} indicator could be used for comparing two VTEC maps. A higher MLH_{Norm} means stronger consistency between the two models.

4. EGNOS PROTECTION LEVEL

The Protection Level (PL) is calculated according to the Radio Technical Committee for Aeronautics (RTCA) [5] [16]. The values of Protection Levels are calculated based on the following formula:

$$HPL = K_H d_{major} \quad (10)$$

$$VPL = K_V d_U \quad (11)$$

where K_H is the bounding factor of user's horizontal position with a probability of 10^{-9} (for en-route navigation K_H = 6.18 and precision approach K_H = 6.0), K_V is the bounding factor of the user's vertical position with a probability of 5×10^{-7} (K_V = 5.33)

$$d_{major} = \sqrt{\frac{d_E^2 + d_N^2}{2} + \sqrt{\left(\frac{d_E^2 - d_N^2}{2}\right)^2 + d_{EN}^2}} \quad (12)$$

$$d_E^2 = \sum_{i=1}^{n} S_{E,i}^2 \sigma_i^2 \quad (13)$$

$$d_N^2 = \sum_{i=1}^{n} S_{N,i}^2 \sigma_i^2 \quad (14)$$

$$d_U^2 = \sum_{i=1}^{n} S_{U,i}^2 \sigma_i^2 \quad (15)$$

$$d_{EN}^2 = \sum_{i=1}^{n} S_{E,i} S_{N,i} \sigma_i^2 \quad (16)$$

$$\boldsymbol{S} = \begin{bmatrix} S_{E,1} & S_{E,2} & \cdots & S_{E,n} \\ S_{N,1} & S_{N,2} & \cdots & S_{N,n} \\ S_{U,1} & S_{U,2} & \cdots & S_{U,n} \\ S_{t,1} & S_{t,2} & \cdots & S_{t,n} \end{bmatrix} \quad (17)$$

where $\boldsymbol{S}$ is the design matrix, d_E^2, d_N^2, d_U^2 are the variances of the East, North and Up (vertical) component of the position solution expressed in a topocentric system, d_{EN} is the covariance between East and North axis, $S_{E,i}$ is the partial derivative of position error in the east direction with respect to the pseudorange error on the i[th] satellite, $S_{N,i}$ is the partial derivative of position error in the north direction with respect to the pseudorange error on the i[th] satellite, $S_{U,i}$ is the partial derivative of position error in the up (vertical) direction with respect to the pseudorange error on the i[th] satellite,

$$\sigma_i^2 = \sigma_{i,flt}^2 + \sigma_{i,UIRE}^2 + \sigma_{i,air}^2 + \sigma_{i,tropo}^2 \quad (18)$$

where σ_i^2 is the full variance of the pseudorange measurement, $\sigma_{i,flt}^2$ is the variance of the residual error after application of fast and slow corrections, $\sigma_{i,UIRE}^2$ is the variance of the residual error after application of ionospheric correction, $\sigma_{i,air}^2$ is the variance of the contribution of the receiver to the residual error, $\sigma_{i,tropo}^2$ is the variance of the residual error after application of tropospheric correction.

5. STATISTICAL ANALYSIS OF EGNOS MODEL

5.1 Comparison of EGNOS's and CODE's VTEC maps

One of the research's goals was the comparison of the EGNOS ionospheric model and the CODE model. The EGNOS's ionospheric model available in hourly files on EMS was converted to IONEX format; thus, the CODE and EGNOS model became straight comparable. This conversion was done by the GINA program and GPSTK library [17] [18].
For comparison, the available EGNOS corrections were used during the year 2018.

The reference CODE's VTEC maps were subtracted from EGNOS's maps. The mean discrepancy of TEC is extremely low, less than 0.1 TECU, but from the minimum, maximum, and the median's variation from the mean show the presence of extreme values (Table 3).

	Mean	Std	Min	Max	Median
Europe	0.08	3.51	-387.40	35.90	0.20

Table 3. Statistics of EGNOS and CODE ionospheric model TEC discrepancy values in 2018. Values are in TECU.

The mean deviations indicates a good correlation between CODE and EGNOS TEC information. EGNOS model tends to underestimate the ionospheric delay at the edge of the coverage area, at the same time overestimating in the inner territory of the coverage area (Figure 8). However, the deviation from the reference is less than 1 TECU in the continental grid points.

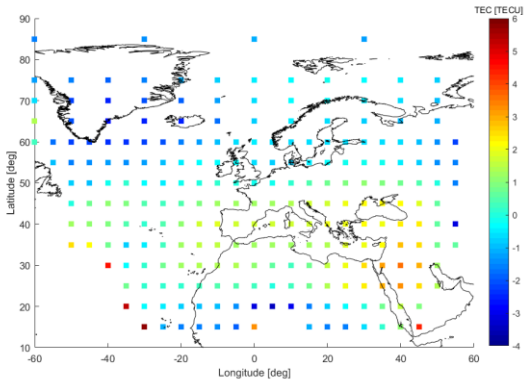

Figure 8. Annual average discrepancies between EGNOS and CODE model in 2018.

The EGNOS ionospheric model's deviation from the CODE model typically is under 4-5 TECU depending on the location, but the outliers could pop up during a yearlong comparison (Figure 9).

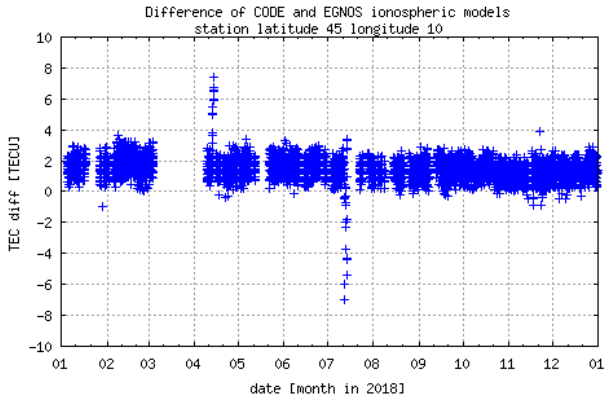

Figure 9. Discrepancies between EGNOS and CODE model at a given grid point.

5.2 MLH COMPARISON OF EGNOS AND CODE GIM

The maximum-likelihood-based method presented in the third chapter was applied to the EGNOS and CODE model. Assuming the two models measure the VTEC values independently, and the RMS values are used as the standard deviation of the Gaussian distribution, the MLH_{Norm} values could be easily calculated. This value had been calculated in common time of the year 2018, in every grid points, then the collected MLH_{Norm} values were averaged (Figure 10).

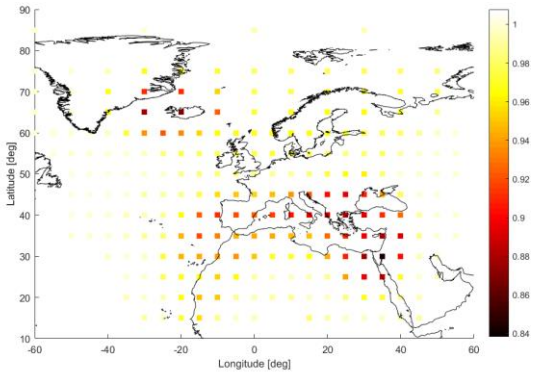

Figure 10. Annual average MLH_{Normed} value from EGNOS and CODE model in 2018

The grid points with the more significant MLH_{Norm} drops can be found around latitude 30° and longitude 35° at the eastern part of the Mediterranean Sea and around Iceland. The MLH_{Norm} tends to be one towards the edge. This tendency is understandable from the fact that the variance of the EGNOS reaches its maximum while for the CODE variances, the order of magnitude is maintained.

The main strength if this MLH comparison is the capability to highlight the area where the two models have the highest consistency.

5.3 Ionospheric effect on the Protection Level

To separate the effect of the ionosphere from other factors, only the $\sigma^2_{i,UIRE}$ term was used to calculate Protection Level. It shall be noted that the Protection Level analyzed in the following section can thus be interpreted as a simulated PL which is significantly lower than the full PL according to Eq. 18. The simulated Protection Level was calculated by the GINA software [18].

The horizontal and the vertical Protection Levels were calculated based on a daily EMS data in separate locations, namely in Budapest, Bucharest, and, Zürich. Besides the Protection Level values, the number of satellites used in positioning is also compared. For the calculations, a 10 degree of elevation cut off angle was used (Figure 11 – 13).

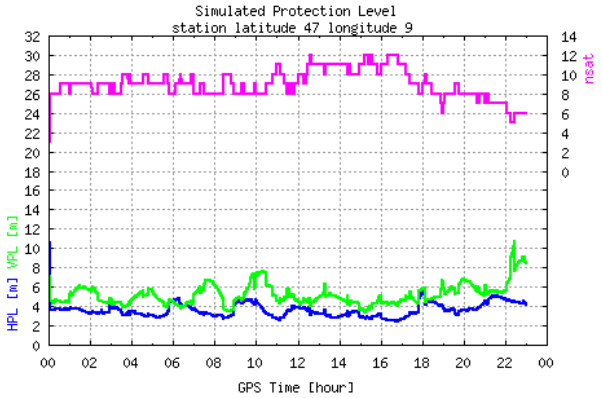

Figure 11. Ionospheric part of the vertical and horizontal Protection Level with the number of satellites. The simulated site is in Zurich on 20/08/2018.

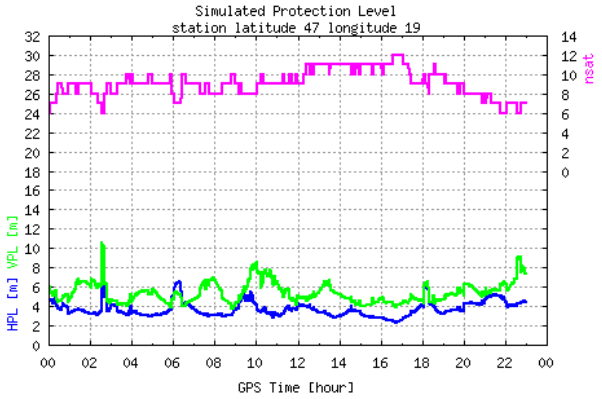

Figure 12. Ionospheric part of the vertical and horizontal Protection Level with the number of satellites. The simulated site is in Budapest on 20/08/2018

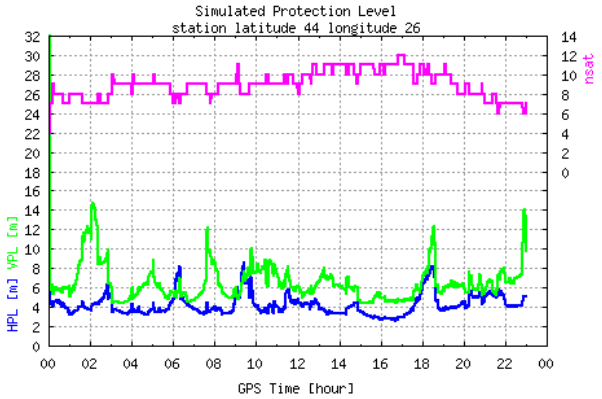

Figure 13. Ionospheric part of the vertical and horizontal Protection Level with the number of satellites. The simulated site is in Bucharest on 20/08/2018

This contribution has been peer-reviewed.
https://doi.org/10.5194/isprs-archives-XLII-4-W14-159-2019 | © Authors 2019. CC BY 4.0 License.

It can be observed that close to the edge of the EGNOS ionospheric model, the ionospheric part of the Protection Level slightly increases (Figure 11 - 13). Near to the edge, the more and more IPP points variances rise drastically, and that is the reason for the effect as mentioned earlier (Figure 14 and 15). The LOS RMS values at the eastern region can exceed 90 TECU while in the inner areas this value remains below 15 TECU.

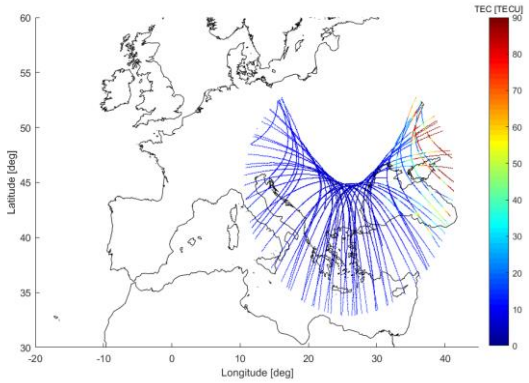

Figure 14. Ionospheric pierce points with line of sight RMS value calculated from the EGNOS VTEC map. The simulated site is in Bucharest on 20/08/2018

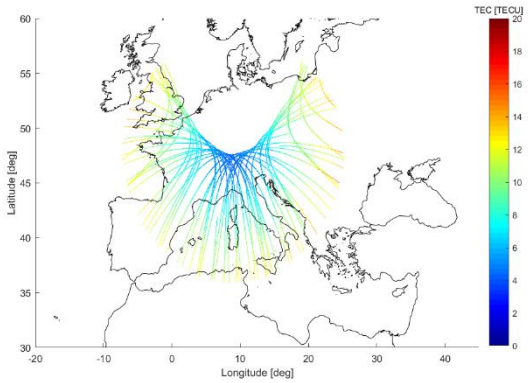

Figure 15. Ionospheric pierce points with line of sight RMS value calculated from the EGNOS VTEC map. The simulated site is in Zürich on 20/08/2018

6. SUMMARY/CONCLUSION

The goal of this article was the examination of the EGNOS ionospheric model. CODE model was used as a reference model since its precision is at least a magnitude better than the EGNOS's model. The differences between the EGNOS ionospheric and CODE model was analyzed using all the available data in 2018. More than 240 grid points were processed in 5500 – 6000 epoch. The discrepancies are small in the continental region of Europe, typically between 0-4 TECU based on the location and time of year. The presence of outliers is observable in any grid point. In extreme cases, the difference could be several tens TECU high.

Leaving the assumption that the CODE model could be handled as a reference, a maximum-likelihood-based method was submitted to analyze the consistency of to VTEC map spatially. Based on this analysis, a significant consistency drop could be found in the region of Iceland and Eastern-South Europe towards the Mediterranean Sea closing with Middle-East.

Finally, the effect of the EGNOS ionospheric model on the Protection Level was demonstrated. Closing to the edge of the broadcasted VTEC map, the increased variances of the grid points have a grand impact on the Protection Level. The Protection Level variations tend to get higher towards the Eastern regions. While in Switzerland the ionospheric horizontal Protection Level remains below 6 meters, in Bucharest the peaks could exceed the 8 meter limit on the same day. The ionospheric vertical Protection Level values show even greater distortion. The reason for this phenomenon is that increased variances of grid points have a notable impact on the Protection Level. More Ranging and Integrity Monitoring Stations at the Eastern regions could mitigate this effect.

REFERENCES

[1] EGNOS Safety of Life (SoL) Service Definition DocumentIssue 3.3

[2] CODE., 2017. Global ionosphere maps produced by CODE. Available from: http://aiuws.unibe.ch/ionosphere/ [Accessed 21 May 2019].

[3] Schaer, S., Gurtner, W., and Feltens, J., 1998. IONEX: The IONosphere Map EXchange Format Version 1, Proceedings of the 1998 IGS analysis centers workshop, 9–11 February 1998 ESOC, Darmstadt, Germany.

[4] Klobuchar, J.A., 1987. Ionospheric time-delay algorithm for single-frequency GPS users. IEEE Transactions on Aerospace and Electronic Systems, AES-23(3), 325–331. doi: 10.1109/TAES.1987.310829

[5] Radio Technical Committee for Aeronautics (RTCA) "Minimum Operational Performance Standards for Airborne Equipment Using Global Positioning System/Wide Area Augmentation System", Doc. DO-229D, 2006, with Change 1, 2013, Washington, DC. URL: http://www.rtca.org

[6] Grunwald, G., Bakuła, M., Ciećko, A., Kaźmierczak, R., 2018. Examination of GPS/EGNOS integrity in north-eastern Poland. *IET Radar, Sonar & Navigation*. 10(1), pp. 114-121. https://doi.org/10.1049/iet-rsn. 2015.005

[7] Grunwald, G., Ciecko, A., Tanajewski, D., 2019. Analysis of Applying the EGNOS System in APV-1 and LPV- 200 Operations. *IOP Conference Series: Earth and Environmental Science*. 221. 012075. 10.1088/1755-1315/221/1/012075.

[8] Prakanrattana, K., Satirapod, C., 2018.
Comparative study of using different ionosphere models in Thailand for single-frequency GNSS users, *Survey Review*. 1-6. 10.1080/00396265.2018.1426260.

[9] Ciećko, A., Grunwald, G. 2017. Examination of Autonomous GPS and GPS/EGNOS Integrity and Accuracy for Aeronautical Applications. *Periodica Polytechnica Civil Engineering*, *61*(4), 920-928. https://doi.org/10.3311/PPci.10022

[10] Bhuiyan, M. Z. H., Kuusniemi, H., Soderini, A., Honkala, S., Marila, S., 2017. Performance of EGNOS in North-East European Latitudes. *Conference: International Technical Meeting of Institute of Navigation At: California, USA* 10.33012/2017.14881.

[11] Ibanez, D., Rovira G., A., Sanz, J., Juan, J., Gonzalez-Casado, G., Jimenez-Banos, D., Lopez-Echazarreta, C., Lapin, I.,

2018. The GNSS Laboratory Tool Suite (gLAB) updates: SBAS, DGNSS and Global Monitoring System. *Conference: 2018 9th ESA Workshop on Satellite Navigation Technologies and European Workshop on GNSS Signals and Signal Processing (NAVITEC) At: ESA ESTEC, Noordwijk, The Netherlands*, 1-11. 10.1109/NAVITEC.2018.8642707.

[12] Pajares, M., Juan, J., Sanz, J., Orús Pérez, R., García-Rigo, A., Feltens, J., Komjathy, A., C., Schaer, S., Krankowski, A., 2008. The IGS VTEC maps: A reliable source of ionospheric information since 1998. *Journal of Geodesy*. 83. 263-275. 10.1007/s00190-008-0266-1.

[13] Prats, X., Orús Pérez, R., Sanz, J., Farnworth, R., Soley, S., 2003. SBAS ionospheric performance evaluation tests.

[14] Markovits-Somogyi, R., Takács, B., de la Fuente, A., Lubrani, P., 2017. Introducing E-GNSS navigation in the Hungarian Airspace. The BEYOND experience and the relevance of GNSS monitoring and vulnerabilities. *3rd International Conference on Research, Technology and Education of Space (H-SPACE 2017) At: Budapest, Hungary*

[15] Dach, R., Schaer, S., Lutz, S., Meindl, M., Bock, H., Orliac, E., Prange, L., Thaller, D., Mervart, L., Jäggi, A., Beutler, G., Brockmann, E., Ineichen, D., Wiget, A., Weber, G., Habrich, H., Söhne, W., Ihde, J., Steigenberger, P., and Hugentobler, U., 2012, Center for Orbit Determination in Europe (CODE). *IGS Technical Report* 2012, 35-46, Jet Propulsion Laboratory.

[16] Takács B., Siki Z., Markovits-Somogyi R., Extension of RTKLIB for the Calculation and Validation of Protection Levels *International Archives of Photogrammetry and Remote Sensing* (2002-)
XLII-4/W2: pp. 161-166. (2017) FOSS4G-Europe 2017. Marne-la-Vallée, France: 2017.07.18 -2017.07.22.

[17] Tolman B., Benjamin Harris R., Gaussiran T, Munton D., Little J., Mach R.,Nelsen S., Renfro B., ARL:UT; Schlossberg D., University of California Berkeley. The GPS Toolkit - *Open Source GPS Software. Proceedings of the 17th International Technical Meeting of the Satellite Division of the Institute of Navigation* (ION GNSS 2004). Long Beach, California. September 2004

[18] Lupsic B., 2019., *GINA - Global Integrated Navigation Algorithm*, - https://github.com/GINAProject (1 June 2019).

[19] Rózsa Sz., 2018, A new approach for assessing tropospheric delay model performance for safety-of-life GNSS applications In: A, Heck; K, Seitz; T, Grombein; M, Mayer; J, -M Stövhase; H, Sumaya; M, Wampach; M, Westerhaus; L, Dalheimer; P, Senger (Hrsg) (szerk.) (SchW)Ehre, wem (Schw)Ehre gebührt : Feitschrift zur Verabschiedung von Prof. Dr.-Ing. Dr. h.c. Bernhard Heck Karlsruhe, Germany : KIT *Scientific Publishing*, pp. 229-235. , 7 p.